



Characterization of Solution Blow Spun Poly(Lactic) Acid Based Nanofibers Containing Sucuk Spice Mix Essential Oils

Iklima Ozcan¹ · Furkan Turker Saricaoglu² · Mahmud Ekrem Parlak² · Adnan Fatih Dagdelen² · Aycan Yigit Cinar² · Latife Betul Gul³ · Ayse Neslihan Dundar² · Fatih Tosun⁴

Accepted: 1 January 2023 / Published online: 13 January 2023

© The Author(s), under exclusive licence to Springer Science+Business Media, LLC, part of Springer Nature 2023

Abstract

In this study, essential oil (EO) from sucuk spice mix was incorporated into poly(lactic) acid (PLA) and nanofibers were produced via solution blow spinning (SBS). EO incorporation was performed at 0, 5, 10, 15, 20, 25, and 30% (v/w) of PLA. Mechanical, barrier, microstructural, topographical, contact angle, chemical, thermal, antioxidant, and antibacterial properties against *E. coli* and *S. aureus* were characterized. Nanofibers were not soluble in water due to the hydrophobic nature of PLA. Microstructural images revealed that beadles and uniform nanofibers can be produced with SBS, and EO addition decreased the average fiber diameter. The surface topography of nanofibers was improved by increasing EO concentration. Melting and glass transition temperatures decreased and the thermal stability of nanofibers increased with EO addition. Nanofibers containing EO at 30% had the highest antioxidant capacity (40.02%). Nanofibers containing 20, 25, and 30% of EO had greater growth inhibition against *Staphylococcus aureus* and *Escherichia coli*. As a result, PLA-based nanofibers containing sucuk spice mix EO can be produced with SBS, and nanofibers containing 20, 25, and 30% EO could be a promising system not only in drug delivery systems but also in food packaging.

Keywords Nanofiber · Food packaging · Solution blow spinning · Poly(lactic) acid · Antibacterial activity

Introduction

Nano-technological developments in recent years have led to produce new materials for biomedical applications such as tissue engineering, wound dressing and controlled release of drugs, and active food packaging applications [1, 2]. One of the most widely investigated Nanomaterial is nanofiber because it has unique properties such as a large surface area

to volume ratio, high encapsulation efficiency, low specific gravity, and controlled-release properties [3]. The production of nanofibers can be achieved by several methods including melt spinning, melt blowing, and electrospinning (ES) from which ES is the most widely studied method due to its adaptability to a wide range of polymeric materials and consistency in producing very fine fibers [4]. In the ES process, a polymeric solution is pumped towards a large electrical field to overcome surface tension, and hence, a fluid jet occurs and travels through the grounded collector. The use of a large electrical field and conductive collector, and a relatively low nanofiber production rate limit the commercialization and the use for an immediate in-situ application of electrospun nanofibers [5].

Recently, a novel alternative nanofiber production technique is developed by Medeiros et al. [3] as solution blow spinning (SBS). In this technique, a concentric nozzle is used through which polymer solution and pressurized gas are simultaneously passed. The aerodynamic drag and shear forces caused by the pressurized gas exiting the nozzle are combined to form a Taylor cone-like shape at the nozzle tip, which is formed in the electrospinning process.

✉ Furkan Turker Saricaoglu
furkan.saricaoglu@btu.edu.tr

¹ AEP Anadolu Etap Penkon Food and Agriculture Products Industry and Trade. Inc., 20600 Denizli, Turkey

² Department of Food Engineering, Faculty of Engineering and Natural Science, Bursa Technical University, 16310 Bursa, Turkey

³ Department of Food Engineering, Faculty of Engineering, Giresun University, 28200 Giresun, Turkey

⁴ Department of Agricultural Economy and Project Management, General Directorate of Agricultural Research and Policy, Republic of Turkey Ministry of Agriculture and Forestry, 06800 Ankara, Turkey

During the flight of polymeric solution towards to collector placed at a fixed distance, the solvent evaporates and the polymer is formed a reticulated yarn structure at the micro and nanoscale, called nanofiber. SBS can be successfully used for the production of nanofibers from poly-lactic acid (PLA) [6–8], poly-lactic co-glycolic acid (PLGA) [5], fish skin gelatin [9], corn zein [10] and poly-methyl methacrylate (PMMA) [3].

Biomedical applications such as wound dressing, tissue scaffolding, drug delivery, and food packaging applications of nanofibers are focused on biodegradable polymers. In this regard, PLA is one of the most promising polymers due to its biodegradability, nontoxicity, well processes ability, and good mechanical properties [11]. In addition, PLA can be processed into fibers that are ideal for the controlled release of encapsulated volatile compounds such as EOs due to their extremely high surface area. PLA-based nanofibers containing linalool [12], copaiba oil [13], and terpinene 4-ol [14] were produced with SBS.

Sucuk is the most widely consumed fermented meat product in Turkey, and it consists of different spices mainly cumin, red pepper, and black pepper. This spice mix is responsible for the main aroma of sucuk after the aromatic compounds are formed by fermentation. It is well known that EOs from spices are natural preservatives that have high antioxidant capacities and antimicrobial activities against most food-pathogenic bacteria. The addition of EOs into biodegradable nanofibers for food packaging applications is a very trendy topic in the literature. Aytac et al. [1] reported that thymol-enriched zein nanofibers could be used for the enhancing shelf life of chicken meat. In another study, PLA nanofibers were enriched with guar gum and thyme EO, and it was stated that these nanofibers could be a promising system in the safety and shelf life of foods [15].

To the best of our knowledge, there is no study focusing on the production of solution blow spun PLA nanofibers incorporated with sucuk spice mix EO. This study mainly aimed to develop sucuk spice mix EO-loaded PLA-based nanofibers with SBS and to characterize the packaging properties of nanofibers in terms of mechanical, barrier, microstructural (SEM), topographical (AFM), chemical (XRD and FTIR), thermal (DSC and TGA), antioxidant, and antibacterial properties.

Materials and Methods

Materials

Poly-lactic acid (PLA) pellets ($M_w = 75.000$ g/mol, $T_g = 65$ – 75 °C, Density@25 °C = 1.24 g/cm³) were purchased from Natureworks (Minnetonka, MN, USA). Before dissolving PLA pellets, residual moisture was

removed by holding pellets for 24 h in an air-circulating oven at 40 °C. The spice mix of sucuk containing 46.88% cumin, 46.87% red pepper, and 6.25% black pepper was kindly provided from Köfteci Yusuf (Bursa, Turkey). The extraction of EOs from the spice mix was carried out with a Clevenger-type (Sesim Chemical Laboratory, Ankara, Turkey) hydro-distillation method. For this purpose, 50 g of spice mix was mixed with 500 g of distilled water in a distillation balloon and boiled for 5 h under reflux. The extracted EOs were dehydrated with sodium sulfate anhydrous and stored in a dark bottle at 4 °C. Chloroform used for the dissolving of pellets, 2,2-Diphenyl-1-picrylhydrazyl (DPPH), and methanol for antioxidant activity were purchased from Sigma-Aldrich (Germany) at analytical grade.

Preparation of Polymer Solutions

The polymer solutions were prepared by combining 5 g of PLA with chloroform (100 mL) in a screw cap glass bottle and the mixture was held on a magnetic stirrer until completely dissolved (~6 h). After the dissolution of PLA, spice mix EO was added at 0 (control), 5, 10, 15, 20, 25, and 30% depending on the PLA concentration, and the solution was mixed additional 30 min. The polymer solution was transferred into a 20 mL syringe and connected to the syringe pump (New Era, NE-4000 model, USA) of the SBS system.

Solution Blow Spinning (SBS)

The nanofiber production system with the SBS technique consists of four main parts: a gas unit as compressed air, a syringe pump to control the injection rate of polymer solutions, the spinning apparatus consisting of a setup of concentric nozzles, and the static plate collector coated with aluminum foil. The feeding rate, air pressure, and collector distance were set based on preliminary experiments (data not shown) as 120 μ L/min, 0.15 MPa (air velocity 7.3 m/s), and 30 cm, respectively. Nanofiber production equipment was settled in a fume hood to prevent the nanofibers from dispersing in the air at which temperature and humidity were 23 °C and 52%, respectively. The air coming out of the compressor was used by passing through a dehumidifier and thus the humidity of the air was minimized. The schematic illustration of SBS and concentric nozzles were reported earlier by Medeiros et al. [3]. The inner nozzle was positioned 2 mm beyond the outer nozzle and the distance between the nozzles was 0.5 mm. The obtained nanofibers were wrapped with aluminum foil and stored in a Ziploc freezer bag in a desiccator.

Characterization of Nanofibers

Water Solubility

The water solubility of nanofibers was determined at room temperature according to Pelissari et al. [16] with slight modifications. For this purpose, 20 mg of nanofiber was mixed with 20 mL of distilled water at 25 °C on a magnetic stirrer for 24 h. Then, the mixture was filtered and the permeant was dried in an oven at 105 °C up to constant weight. The water solubility of nanofibers was determined from the residue after evaporation.

Mechanical Properties

The tensile properties (tensile strength and elongation at break) of nanofibers were determined with a TA-HD Plus Texture analyzer (Stable Micro Systems Co, Ltd., Godalming, UK) based on ASTM standard method [17]. Nanofiber sheets conditioned at 53% relative humidity were cut into strips (1 cm width × 8 cm length) and fixed to mini tensile grips. The initial gap between the tensile grips was fixed to 6 cm, and the probe speed was arranged as 2 mm/s until the break of strips. The stress–strain curves of nanofibers were used for the calculation of tensile strength (TS) and elongation at break (EAB), and at least eight nanofiber strips were tested for all samples.

The burst strength (BS) and deformation (BD) of nanofibers were also investigated with a Texture Analyzer equipped with a film support ring with a 10 mm diameter and nanofibers were cut into a rectangular shape as 3 cm × 3 cm. The ball probe at 6.25 mm diameter (SMS P/0.25S) was moved through the center point of the ring at 0.2 mm/s test speed. The maximum force to rupture the film sample was recorded, as well as the maximum distance before rupture, and all the nanofibers were tested at least in triplicate [18].

Water Vapor Permeability (WVP)

The water vapor permeability (WVP) of nanofibers was determined using the gravimetric modified cup method as described by McHugh et al. [19] based on the ASTM E96–80 method. Nanofiber sheets were cut into a circular shape in 80 mm diameter and a digital micrometer (Mitutoyo Manufacturing) was used for determining the thickness at five different locations of nanofibers. The nanofibers were attached to poly (methyl methacrylate) cups with a 50 mm diameter opening filled with 6 mL of distilled water. Three different cups for each type of nanofiber were placed in a cabinet containing anhydrous silica (0% relative humidity). The water loss of cups was recorded every 2 h intervals with

an analytical balance, and the WVP of nanofibers was calculated as $\text{g}\cdot\text{mm}/\text{m}^2\cdot\text{h}\cdot\text{kPa}$.

Scanning Electron Microscopy and Fiber Diameter

Nanofibers were cut into small pieces and glued onto aluminum stubs with a double-sided adhesive carbon band. Then, samples were coated by a sputter coating (Leica, EM ACE600 model, USA) with gold–palladium at 25 mA. Nanofibers were visualized by field emission scanning electron microscopy (SEM) (Carl Zeiss, Gemini SEM360 model, Germany) at an accelerated voltage of 10 kV. The SEM micrographs of nanofibers were further analyzed by ImageJ software to calculate fiber diameter distribution from at least 100 random measurements and the average fiber diameter was also determined with a Gaussian curve to fit by OriginLab software (OriginPro 8.5 version, USA).

Atomic Force Microscopy (AFM)

The surface topography of nanofibers was visualized with atomic force microscopy (Nanosurf, Flex AFM model, Switzerland). A rectangular cantilever with a spring constant of 20–60 N/m was positioned over the sample, and 15 μm × 15 μm images were captured from the samples. The roughness of samples was statistically calculated by device software based on the average of the absolute value of the height deviations from a mean surface, R_a , and the root-mean-square average of height deviations taken from the mean data plane, R_q .

Contact Angle Measurement

The wettability of nanofibers enriched with EO was determined by a sessile-drop method using contact angle measurement (Athension Theta, Biolin Scientific, Sweden). Distilled water (5 μL) was dropped onto nanofibers, and then the contact angle between the drop and surface of nanofibers was measured and the related images were captured.

Thermal Properties

The thermal properties of nanofibers were characterized using differential scanning calorimeter (DSC) and thermogravimetric analyses (TGA). Before DSC and TGA analyses, nanofibers were conditioned for 3 weeks in a desiccator containing silica. Nanofibers (4–5 mg) were analyzed under a nitrogen atmosphere at a flow capacity of 20 mL/min with a DSC device (TA Instruments, Discovery DSC251 model, USA). Temperature scanning ranged from – 40 to 200 °C at a heating rate of 5 °C/min. For TGA, approximately 10 mg of nanofiber was weighed and scanned from 20 to 600 °C at a heating rate of 10 °C/min with a TGA device

(TA Instruments, SDT650 model, USA) under nitrogen as purge gas at 20 mL/min flow rate.

X-ray Diffraction (XRD)

The effect of EO incorporation on the crystallinity of PLA nanofibers was determined with a wide-angle XRD device (Bruker, AXS Discovery D8, MA, USA) equipped with Cu-K α radiation source ($\lambda = 1.546 \text{ \AA}$). The incidence angle as 2θ ranged from 4 to 40° at a scanning rate of 2° min⁻¹. All samples were held in a desiccator containing silica for 2 weeks to remove moisture.

FTIR Spectrum

The FTIR spectrum of nanofibers containing EOs was determined using an FTIR device (TA, Nicolet iS50, CA, USA). The samples were directly placed in the sample chamber of the device and the spectrums were taken directly with the help of an ATR diamond crystal at a scan resolution of 2 cm⁻¹ between the wavenumber range from 4000 to 400 cm⁻¹. All samples were stored in a desiccator with silica for minimizing the moisture content of the samples.

Antioxidant Capacity

The antioxidant capacity of nanofibers enriched with spice mix EO was determined with the 2,2-diphenyl-2-picrylhydrazyl (DPPH) scavenging activity. For this purpose, 100 mg of nanofiber was mixed with 5 mL of methanol in a centrifuge tube and held in a shaking water bath at 25 °C for 2 h. Samples were then centrifuged at 5000×g for 10 min and 0.5 mL of supernatant was vigorously mixed with 3.5 mL of 0.06 mM DPPH and held for 30 min in a dark environment. The absorbance of the solution was measured at 517 nm with a spectrophotometer (Rigol, Ultra 3660 model, India). The DPPH scavenging activity was calculated with the following equation:

$$AC(\%) = \frac{Abs_{Control} - Abs_{Sample}}{Abs_{Control}} \times 100 \quad (1)$$

where AC is the antioxidant capacity, $Abs_{Control}$ is the absorbance of the DPPH solution and Abs_{Sample} is the absorbance of test samples.

Antibacterial Activity

The antibacterial activity of nanofibers against *E. coli* ATCC35218 and *S. aureus* ATCC6538 was evaluated for the control and samples containing 25 and 30% spice mix EOs which had the lowest fiber diameters, better surface topography, and the highest antioxidant capacity. The Agar disc

diffusion method did not show inhibition zones probably due to the hydrophobic properties of PLA-based nanofibers. Therefore, the bacterial colony counting method was carried out as described earlier by Lin et al. [20] for nanofibers. For this purpose, 400 mg of nanofibers were cut with a sterile razor blade and each surface of nanofibers was held in a UV cabin for 30 min to sterilize the surface. *S. aureus* and *E. coli* were firstly incubated in Mueller Hinton broth at 37 °C for 24 h and inoculum was re-suspended to provide a final density of 5.0×10^5 CFU/mL in phosphate-buffered saline according to 0.5 McFarland turbidity standard. The sterilized nanofibers (~400 mg) were immersed in bacterial suspension in 20 mL of conical falcon tubes, and tubes were incubated in a shaker at 37 °C for 24 h. Dilutions between 10^1 and 10^9 were prepared by adding 1 mL culture into 9 mL of phosphate buffer saline solution, and then, 0.1 mL of the diluted culture were spread onto a Mueller Hinton agar plate and incubated at 37 °C for 24 h. The colony-forming unit (CFU) were counted and the antibacterial activity of nanofibers was defined as the following equation:

$$Antibacterial\ activity(\%) = \frac{A - B}{A} \times 100 \quad (2)$$

where A and B are the number of colonies before and after nanofibers are added, respectively [1].

Statistical Analysis

The production process of nanofibers was repeated three times and all analyses were performed at least in duplicate. The results were analyzed by one-way analysis of variance (ANOVA) using the SPSS 21.0 package program (IBM, Chicago, IL, USA) and results were presented as mean \pm standard deviation. Significant differences between the means were evaluated with Duncan's multiple range test at a significance value of $p < 0.05$.

Results and Discussions

Water Solubility

The water solubility of nanofibers is crucial in pharmacy, whereas insoluble nanofibers are desired for packaging applications. The effect of EO incorporation on the water solubility of PLA-based solution blow-spun nanofibers is summarized in Table 1. PLA-based nanofibers displayed low water solubility between 3.79 and 17.78 mg/L, probably due to the hydrophobic nature of PLA and EO. However, the increase of EO concentration significantly increased the water solubility of nanofibers, except for 25% EO concentration, which showed a similar value with 10% EO addition, and the highest water solubility was observed from 30%

Table 1 Water solubility and mechanical properties of solution blow spun nanofibers enriched with sucuk spice mix essential oil

Samples	WS (mg/L)	TS (MPa)	EAB (%)	BS (N)	BD (mm)
Neat PLA	3.79 ± 0.30 ^e	0.49 ± 0.05 ^a	118.13 ± 1.48 ^c	26.11 ± 1.25 ^a	1.25 ± 0.06 ^b
PLA + 5% EO	4.07 ± 0.09 ^e	0.48 ± 0.05 ^a	119.09 ± 2.88 ^{bc}	21.11 ± 1.40 ^c	1.21 ± 0.02 ^b
PLA + 10% EO	5.17 ± 0.24 ^d	0.43 ± 0.03 ^b	119.85 ± 1.95 ^{abc}	21.09 ± 1.61 ^c	1.20 ± 0.07 ^b
PLA + 15% EO	7.03 ± 0.04 ^c	0.38 ± 0.05 ^{bc}	120.36 ± 1.56 ^{abc}	25.71 ± 1.78 ^a	1.26 ± 0.07 ^b
PLA + 20% EO	8.02 ± 0.03 ^b	0.36 ± 0.04 ^c	120.61 ± 2.02 ^{abc}	19.16 ± 0.74 ^d	1.04 ± 0.05 ^c
PLA + 25% EO	5.03 ± 0.04 ^d	0.34 ± 0.03 ^{cd}	121.54 ± 3.26 ^{ab}	22.90 ± 1.07 ^b	1.23 ± 0.05 ^b
PLA + 30% EO	17.78 ± 0.31 ^a	0.31 ± 0.05 ^d	122.41 ± 3.02 ^a	23.56 ± 1.44 ^b	1.32 ± 0.04 ^a

Values are mean ± standard deviation

WS: Water solubility; TS Tensile strength; EAB Elongation at break; BS Burst strength; BD Burst deformation; PLA Polylactic acid; EO Essential oil obtained from sucuk spice mix

^{a–e}Means within the same column with different letters are different ($p < 0.05$)

EO added nanofibers. The low water solubility of solution blow spun nanofibers could be attributed to the hydrophobic nature of PLA. EOs are also hydrophobic, but the increasing concentration of EOs caused the migration to water during the solubility test, and hence increased the water solubility results, except for 25% EO added nanofibers.

Mechanical Properties

The mechanical properties of polymer materials, either film or nanofiber sheet, are considered a key factor in packaging applications, and the mechanical behavior of nanofiber sheets depends highly on processing conditions, composition, fiber structure, interactions between fibers, and individual properties of fiber constituents [21]. Tensile strength (TS), elongation at break (EAB), burst strength (BS) and burst deformation (BD) results of solution blow spun nanofibers enriched with sucuk spice mix EO are summarized in Table 1. The TS values of solution blow spun nanofibers significantly decreased with increasing EO addition, and the neat PLA nanofibers showed the highest TS value, while the nanofibers enriched with 30% EO had the lowest TS value. The decreasing trend of TS values could be attributed to the average fiber diameter, which decreased with increasing EO incorporation. The addition of EO improved the EAB values probably due to the plasticizer effect of EO, and a similar situation was also observed from the BD values. The BS values of nanofibers display the strength of nanofiber sheets against vertical forces, and the increasing EO content significantly decreased the BS values, except for the 15% EO added sample which showed similar BS value with neat PLA nanofiber sheet, probably due to similar fiber diameters. The obtained mechanical results were also in accordance with the atomic force microscopy results, in which the addition of EO resulted in a higher surface roughness, and therefore mechanical properties decreased with increasing EO. In addition, the crystallinity of nanofibers generally increased when compared to neat

PLA nanofiber, except for 10% EO addition, and the highest crystallinity was determined from a 15% EO incorporated sample (Table 3), which supported to higher BS value. Our results were also in accordance with the results of Promnil et al. [22] who determined the mechanical properties of electrospun PLA nanofibers.

Water Vapor Permeability

The water vapor permeability (WVP) of a polymer film or nanofiber sheet is an important property when choosing the packaging material to control moisture transfer between the food and the environment. In general, packaging materials with low WVP are preferred for food packaging applications. However, although nanofiber sheets are produced like polymer films, they cannot be expected to have low WVP. Because nanofibers have a porous structure on a nanoscale and water vapor can move through these pores. The WVP of neat PLA and EO-incorporated PLA nanofiber sheets is summarized in Table 2. The neat PLA nanofibers showed the highest WVP, and the incorporation of EO into nanofibers significantly decreased the WVP, and the lowest value was observed from the 30% EO incorporated nanofiber sheet ($p < 0.05$). The surface hydrophobicity and morphology of nanofibers could directly be attributed to WVP, as well as average fiber diameter and crystallinity. The hydrophobic structure of the PLA and hydrophobicity of EO, and surface roughness of nanofibers were in accordance with the barrier properties against water vapor. Moreover, the increasing crystallinity with increasing EO addition also improved the barrier properties of nanofibers via behaving as a nucleating element and occurring in impermeable regions onto nanofiber sheets [23]. In a study conducted by Yang et al. [24] the WVP of solution blow spun gelatin nanofibers was determined higher than our results, due to the hydrophilic structure of gelatin. In another study, the incorporation of EO into electrospun poly-vinyl alcohol (PVA) nanofibers increased the WVP, and this increase was related to the

Table 2 Water vapor permeability, antioxidant capacity, average fiber diameter and surface roughness factor of solution blow spun nanofibers enriched with sucuk spice mix essential oil

Samples	WVP	AC (% inhibition)	AFD (nm)	R _a (nm)
Neat PLA	2.113 ± 0.008 ^a	-	71.15 ± 6.34 ^c	331
PLA + 5% EO	2.040 ± 0.027 ^b	26.56 ± 0.01 ^f	78.93 ± 2.46 ^c	399
PLA + 10% EO	1.956 ± 0.017 ^c	28.29 ± 1.76 ^e	109.35 ± 4.47 ^a	381
PLA + 15% EO	1.910 ± 0.005 ^d	31.14 ± 0.31 ^d	79.13 ± 1.81 ^c	356
PLA + 20% EO	1.848 ± 0.014 ^e	34.79 ± 0.01 ^c	92.74 ± 1.04 ^b	256
PLA + 25% EO	1.814 ± 0.006 ^f	36.38 ± 0.02 ^b	63.17 ± 1.81 ^d	295
PLA + 30% EO	1.552 ± 0.014 ^g	40.02 ± 2.78 ^a	58.17 ± 3.80 ^d	590

Values are mean ± standard deviation

WVP Water vapor permeability (g.mm/m².h.kPa); AC Antioxidant capacity; AFD Average fiber diameter; R_a Surface roughness factor; PLA Polylactic acid; EO Essential oil obtained from sucuk spice mix

^{a–g}Means within the same column with different letters are different ($p < 0.05$)

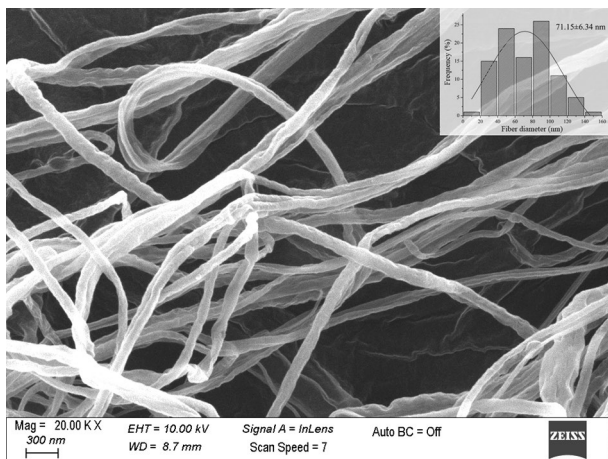


Fig. 1 Scanning electron microscope image of neat PLA nanofibers obtained with solution blow spinning

increasing hydrophilicity of nanofibers due to the emulsification process [25].

SEM Analysis

The production of PLA-based nanofibers with the SBS process was successfully achieved on a nanometer scale. The microstructure of neat (control) and EO-enriched PLA nanofibers, as well as fiber diameter distribution, are depicted in Figs. 1 and 2, respectively. The neat PLA nanofibers showed a rough surface when compared with EO-enriched nanofibers. As reported earlier by Oliveira et al. [6], the viscosity of polymer solutions is responsible for smooth fiber morphology. SEM micrographs revealed that beads and films as an indicator of poor nanofiber spinning conditions were not observed for all samples. This result indicates that the chosen polymer concentration and spinning variables such as air pressure, working distance, and feed rate, were suitable for the production of nanofibers without beads and films. However, nanofibers enriched

with EO presented a homogeneous aspect (Fig. 2), except for the neat PLA nanofibers (Fig. 1), which displayed a rough nanofiber surface. This could be attributed to the plasticizing effect of EO [14] and the evaporation rate of polymer solution, in which EO addition changed the evaporation rate of solutions [26]. Similar results were also reported by Bonan et al. [13] who produced PLA-based SBS nanofibers containing Copaiba oil, and by Miranda et al. [26] for polystyrene-based SBS nanofibers with orange oil. The average fiber diameter was significantly affected by the EO incorporation ($p < 0.05$). EO added up to 20% significantly increased the fiber diameter when compared with neat PLA nanofiber. However, nanofibers containing 25 and 30% EO showed the lowest fiber diameter. The final morphology of nanofibers obtained by SBS can mainly be changed by the feed rate, polymer concentration, air pressure, and distance between the nozzle and collector [6]. All these parameters were kept constant, and only EO concentration varied which resulted in the variation of average fiber diameter. The variation in fiber diameter could probably be related with the change in viscosity and evaporation rate of polymer solution. The production of nanofibers from viscous polymer solutions is more difficult, less effective and stable than the viscous solutions which produced from polymers with poor compatibility [7, 8].

Surface Topography

The surface topography of solution-blown spun nanofibers are shown in Figs. 3 and 4 for control and EO enriched, respectively. The surface of nanofibers was the most uneven, but EO incorporation caused a slightly smoother surface, except for 30% addition which resulted in an uneven surface. The surface roughness factor (R_a) of nanofibers without EO was determined as 331 nm, and 5, 10, 15, 20, 25, and 30% EO-incorporated nanofibers showed 399, 381, 356, 256, 295, and 590 nm R_a values, respectively (Table 1). In general, the surface roughness of nanofibers

Fig. 2 The effect of essential oil addition on the morphological structure of PLA nanofibers obtained with solution blow spinning

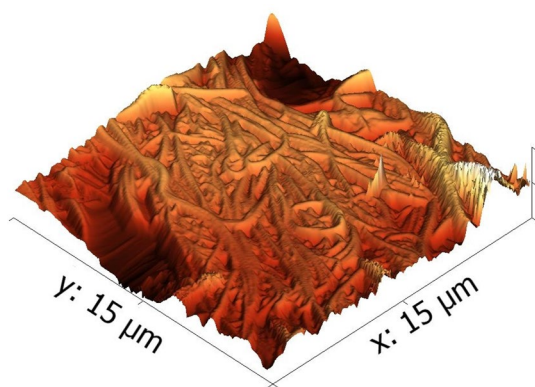
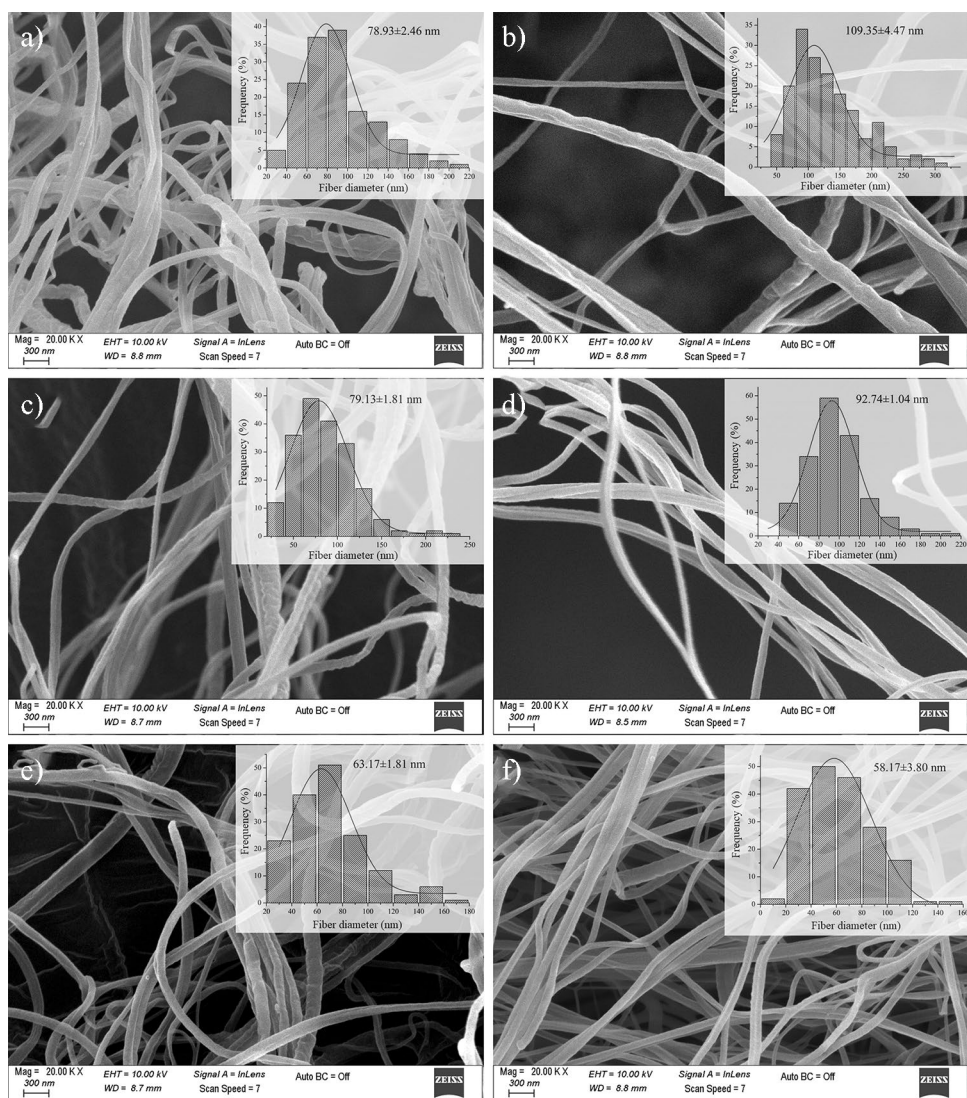
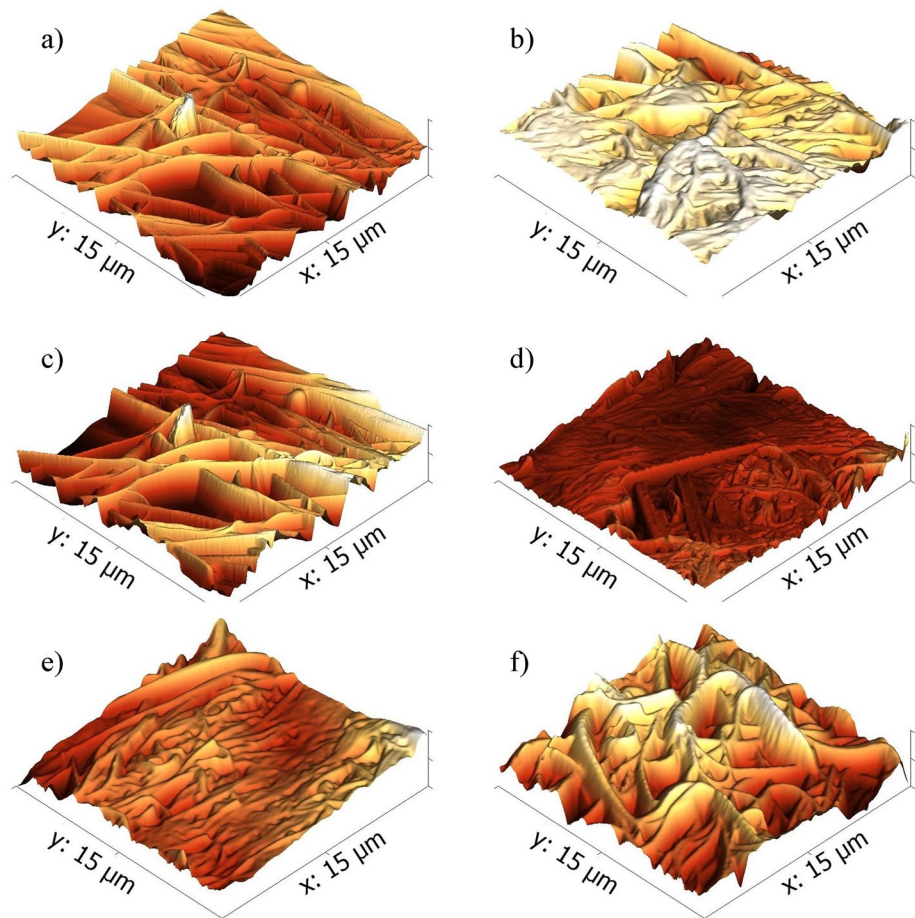


Fig. 3 The surface topography of neat PLA nanofibers obtained with solution blow spinning

is closely related to the average fiber diameter. Although the lowest fiber diameter was observed from the sample containing 30% EO, the highest surface roughness was obtained. Our results showed that the R_a values of nanofibers were similar to values obtained from electrospun nanofibers [27, 28] indicating that SBS is a successful technique for the production of nanofibers in nanoscale. Agrawal and Pramanik [28] stated that the suitable surface roughness of nanofibers for cell attachments and growth in tissue engineering applications should be in the range of 262–435 nm. In another study, the incorporation of chitosan in electrospun PVA nanofibers decreased the surface roughness probably due to lower fiber diameter [29]. However, Milleret et al. [30] reported that the increasing starch ratio in the nanofiber mats increased the fiber diameter and hence surface roughness.

Fig. 4 The effect of essential oil addition on the surface topography of PLA nanofibers obtained with solution blow spinning



Contact Angle

The hydrophilicity or hydrophobicity of a surface can be determined with the contact angle of a water drop, and this analysis gives significant information about the wettability of the surface. If the contact angle is lower than 90° , the surface is wettable, whereas if a higher angle than 90° is observed, the surface is non-wettable and the material is completely hydrophobic. The higher contact angle is generally accepted for food packaging applications due to low water sensitivity and good barrier against water vapor [31]. The surface wettability and hydrophobicity of EO-incorporated PLA nanofibers are illustrated in Fig. 5a. It is well known that PLA contains a large number of hydrophobic ester groups, and therefore all the nanofibers had a hydrophobic surface structure showing a higher contact angle than 100° [32]. Moreover, the increasing ratio of EO from the sukuk spice mix caused an increase in contact angle results and the highest contact angle was observed from the sample containing 30% EO. The addition of hydrophobic compounds such as EOs in the PLA-based nanofibers improved the hydrophobicity and less wettable surfaces were obtained. Furthermore, the crystallinity of solution blow spun PLA

nanofibers was increased based on XRD and DSC results, and the higher the crystallinity, the more difficult the diffusion and transformation of water [33]. Our results were in accordance with the WVP and AFM images, in which WVP decreased and nanofiber sheets became more smooth depending on the EO concentration.

Thermal Properties of Nanofibers

DSC curves of nanofibers with and without EO are illustrated in Fig. 6 and related results are summarized in Table 3. The neat PLA as control displayed glass transition (T_g), crystallization (T_c), and melting (T_m) temperatures of 70.79, 99.66, and 174.16 $^\circ\text{C}$, respectively, which are similar values reported in the literature [13, 14, 34]. These temperatures showed small shifts with the addition of EO at different ratios. In general, T_g and T_c showed a higher decrease with increasing EO concentration when compared to T_m which was similar to the control. The decreasing tendency of T_g and T_c could be explained by the plasticizing effect of EO [12, 14]. EO incorporation into the PLA-based nanofibers may improve the flexibility of PLA, and also affect the crystallinity compared to neat PLA. Souza et al. [12] reported that

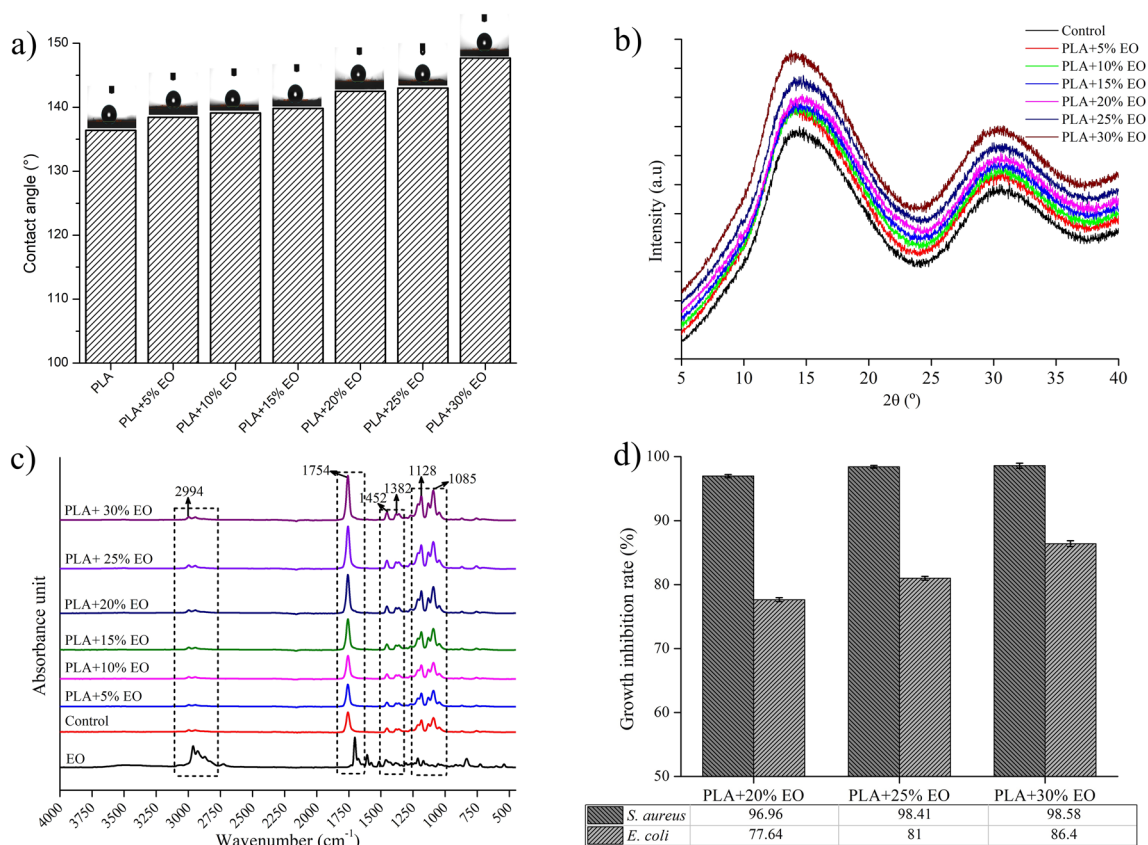


Fig. 5 Contact angle (a), XRD (b), FTIR (c) and antimicrobial properties (d) of solution blow spun PLA-based nanofibers containing various amounts of essential oils

nanofibers produced with SBS showed a higher degree of crystallinity than electrospun nanofibers due to better orientation during the SBS process, and also they stated that this was because solvent evaporation was faster in nanofiber production with SBS.

Another thermal analysis, thermo-gravimetric analysis (TGA) is performed to indicate the thermal decomposition of nanofibers. TGA curves and related results are presented in Fig. 6 and Table 4, respectively. It can be observed that there were two main degradation temperatures for neat PLA and EO-added nanofibers. The first degradation was due to the evaporation of water and EOs, whereas the second degradation was due to the degradation of PLA. The onset temperature of first degradation and related weight loss for control nanofiber was recorded as 46.98 °C and 2.34%, respectively. The addition of EO up to 15% did not affect the onset temperature of the first degradation, but higher concentrations of EO such as 20, 25, and 30% displayed 57.02, 51.16, and 73.77 °C of onset temperatures for the first degradation, respectively. The weight loss of samples at the first decomposition temperature ranged between 0.51 and 6.77%. EO incorporation caused higher weight loss than control, except for the 5% EO added sample, due to evaporation of

water and EO. The main thermal degradation occurred in the second stage, at which the onset temperatures ranged from 195.04 to 246.82 °C, and the weight loss was between 90.31 and 97.46%. The highest weight loss in the second stage was observed from the control, and it decreased with increasing EO incorporation, probably due to the loss of EO in the first stage. The thermal degradation behavior of nanofibers is mainly dependent on the mobility and compactness of polymer chains [15, 35]. The interactions between EO and PLA, the most probable hydrogen bonds, caused the improvement of the regularity and compactness of polymer chains, and hence thermal stability increased [15]. In addition, the increased thermal stability with EO concentration could cause an increasing residue after thermal treatments.

XRD

The effect of EO incorporation on the crystallinity of solution blow spun PLA nanofibers was illustrated in Fig. 5b. The XRD pattern of neat PLA nanofiber exhibited typical broad peaks at 2θ angles around 15° and 30° indicating an amorphous structure. The addition of EO into PLA nanofibers did not cause shifting or occurring new peaks in the

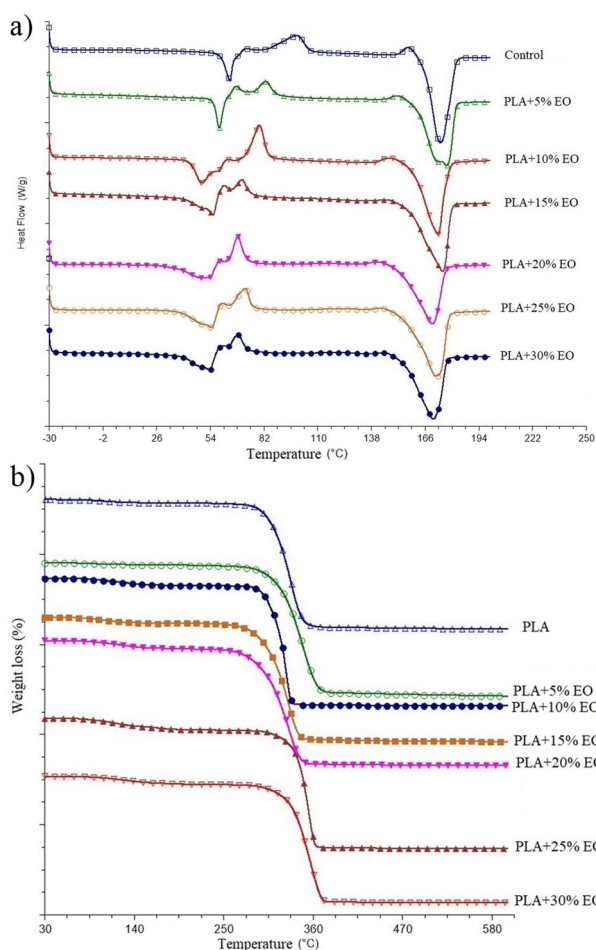


Fig. 6 DSC and TGA curves of solution blow spun PLA-based nanofibers containing various amounts of essential oils

pattern. However, the intensity of the peaks was increased depending on the EO concentration indicating that the crystallinity of the nanofiber sheets obtained by solution blowing decreased probably due to the rapid evaporation of solvent during air pressurizing [36]. A similar observation was reported by Wang et al. [37] for *Perilla* EO-loaded

electrospun PLA nanofibers showing that the crystallinity strength of EO-loaded PLA nanofiber sheets was higher than that of neat PLA nanofibers. This meant that PLA and EOs had good compatibility and did not greatly alter the structural organization of the polymer molecule. These results were well supported by the mechanical and barrier properties of solution blow-spun PLA nanofibers, as well as surface hydrophobicity. Mori et al. [38] found that the XRD patterns of EO-loaded PLA nanofibers did not significantly change and only peak intensity variations were observed.

FTIR Spectrum

FTIR analysis of solution blow spun PLA nanofibers loaded with sucuk spice mix EO was performed for the investigation of intermolecular interactions between PLA and EO, and all the nanofiber sheets displayed a similar spectrum indicating no obvious changes in the molecular and chemical structure after the EO addition (Fig. 5c). The FTIR spectrum of EO from sucuk spice mix revealed multi peaks at the wavenumbers of 2962.28, 2927.42, and 2870.87 cm^{-1} relating with the symmetric and asymmetric $-\text{C}-\text{H}-$ stretching vibrations of hydrocarbons ($-\text{CH}_3-$ and $-\text{CH}_2-$) attached to oxygen (ethers) [39]. The peaks located at 1704.12, 1607.83, 1463.71, 1212.56, and 840.06 cm^{-1} were relevant to aliphatic esters, aromatic cyclohexenes, aromatic cycles, carbonyls, and sulfate esters, respectively [40]. The neat PLA nanofiber displayed characteristic peaks corresponding to $-\text{C}=\text{O}-$ ester carbonyl (1754 cm^{-1}), $-\text{C}-\text{H}-$ deformation (1452 and 1382 cm^{-1}), and $-\text{C}-\text{O}-$ stretching (1128 and 1085 cm^{-1}) [41]. The backbone structure of PLA nanofibers remained constant, but the intensities of some peaks increased depending on the EO addition. For instance, the intensity of the peak at 2994 cm^{-1} increased with EO incorporation, and the main peak of EO at 1704 cm^{-1} shifted to 1754 cm^{-1} for nanofibers, as well as increasing peak intensity. This could be attributed to hydrogen bonding between the amide I bands of PLA and EO. The increasing peak intensities and occurring new peaks for PLA nanofibers

Table 3 Differential scanning calorimetry results of PLA based SBS nanofibers containing sucuk spice mix essential oil

Samples	T_g ($^{\circ}\text{C}$)	ΔH_g (J/g)	T_c ($^{\circ}\text{C}$)	ΔH_c (J/g)	T_m ($^{\circ}\text{C}$)	ΔH_m (J/g)	X_c (%)
Neat PLA	70.79	9.25	99.66	12.09	174.16	50.40	41.19
PLA + %5 EO	65.04	6.74	83.49	5.09	177.28	51.77	50.19
PLA + %10 EO	46.39	15.33	79.64	14.68	172.81	46.38	33.89
PLA + %15 EO	58.15	17.11	71.00	3.51	175.11	54.06	54.35
PLA + %20 EO	56.35	15.53	68.52	8.64	169.76	46.51	40.72
PLA + %25 EO	57.73	16.51	72.82	7.10	171.77	54.38	50.84
PLA + %30 EO	56.68	13.53	68.83	4.29	170.42	51.00	50.23

T_g Glass transition temperature ($^{\circ}\text{C}$); ΔH_g Heat of glass transition (J/g); T_c Crystallization temperature ($^{\circ}\text{C}$); ΔH_c Heat of crystallization (J/g); T_m Melting temperature ($^{\circ}\text{C}$); ΔH_m Heat of melting (J/g). PLA Polylactic acid; EO Essential oil obtained from sucuk spice mix

Table 4 Thermo-gravimetric analysis results of PLA based SBS nanofibers containing sucuk spice mix essential oil

Samples	$T_{d1\ onset}$ (°C)	ΔW_1 (%)	$T_{d2\ onset}$ (°C)	ΔW_2 (%)	Residue (%)
Neat PLA	46.98	2.34	195.04	97.46	0.20
PLA + %5 EY	39.69	0.51	232.70	97.30	2.19
PLA + %10 EY	45.60	5.50	246.82	92.86	1.64
PLA + %15 EY	47.12	4.55	196.72	91.45	4.00
PLA + %20 EY	57.02	6.24	211.38	90.27	3.49
PLA + %25 EY	51.16	6.77	205.01	90.31	2.92
PLA + %30 EY	73.77	5.80	220.85	91.76	2.44

$T_{d1\ onset}$ Onset temperature of the first thermal degradation (°C); $T_{d2\ onset}$ Onset temperature of the second thermal degradation (°C); ΔW_1 Mass loss of the first thermal degradation (%); ΔW_2 Mass loss of the second thermal degradation (%); PLA Polylactic acid; EO Essential oil obtained from sucuk spice mix

incorporated with sucuk spice mix EO indicated that the sucuk spice mix EO could be successfully loaded in solution blow spun PLA nanofibers.

Antioxidant Activity

The oxidation reactions occurring in the food which contact with oxygen cause the deterioration of lipids and the production of free radicals in foods. The scavenging of these free radicals is very important and in this regard, the antioxidant activity of EO-incorporated nanofibers was measured by the DPPH scavenging activity. The EO obtained from the spice mix containing cummin, red and black pepper contains high content of phenolic compounds and therefore displays antioxidant activity. As summarized in Table 2, the neat PLA nanofiber did not have antioxidant activity, whereas the EO incorporation, as expected, significantly increased the antioxidant activity of solution blow spun nanofibers ($p < 0.05$). The increment of EO at 5% caused at least a 4.57% increase in the antioxidant activity of nanofibers. However, the highest amount of EO addition (30%) caused a 50.68% increase in antioxidant activity when compared with the lowest EO addition (5%). Our results were in accordance with the results of Maroufi et al. [15] for electrospun PLA nanofibers enriched with thyme EO.

Antibacterial Activity

The EOs of sucuk spice mix contains various compounds, such as thymol, carvacrol, cummin aldehyde, terpinene, and limonene [42] and it is also well known that these compounds impart antimicrobial activity to EOs against various microorganisms. Due to the hydrophobic nature of PLA and EOs, the agar disc diffusion method did not give results for solution blow spun PLA nanofibers, and antibacterial activity against Gram-negative *E. coli* and Gram-positive *S. aureus* bacteria was evaluated via colony counting method (Fig. 5d). The antibacterial activity of nanofibers containing the highest amount of EO (20, 25, and 30%) was determined

because these nanofibers displayed the highest antioxidant activity and the lowest average fiber diameter (25 and 30%). It is clear in Fig. 5d that the increasing EO concentration in nanofibers significantly increased the growth inhibition of *E. coli*, whereas 25 and 30% EO-incorporated nanofibers showed similar antibacterial activity against *S. aureus*. The increasing concentration of EO caused higher diffusivity in the broth medium, which is consistent with the water solubility results of nanofibers. Moreover, the growth inhibition of nanofibers against *S. aureus* was higher than in *E. coli*. This might be related to the cell wall composition of Gram-negative and Gram-positive bacteria. Thus, *E. coli* has a thin peptidoglycan layer and an outer layer of lipoproteins, lipopolysaccharides, and phospholipids, while the cell wall of *S. aureus* comprises a peptidoglycan layer with lots of pores. The porous cell wall structure of *S. aureus* makes it easy to be permeated by active compounds of EO [43, 44].

Conclusions

In this study, novel solution-blown spun nanofibers containing various amounts of EO were successfully fabricated and the mechanical, water barrier, microstructural, topographical, chemical, thermal, antioxidant, and antimicrobial characterization of nanofibers were performed. The hydrophobic nature of PLA caused fewer water-soluble nanofibers, but higher EO concentration increased the water solubility. Uniform and bead-free nanofibers were obtained by the SBS technique and the addition of EO decreased the average fiber diameter. EO incorporation decreased the surface roughness and caused a smoother surface due to plasticizing effect of EO. The XRD results were well fitted to the mechanical and barrier properties of nanofibers, as well as DSC results. FTIR spectra of neat and EO-loaded PLA nanofibers revealed that PLA nanofibers could be successfully loaded with sucuk spice mix EO. DSC and TGA curves of nanofibers revealed that the melting and glass transition temperatures decreased, whereas the thermal stability of

nanofibers increased with EO addition. Nanofibers containing EO displayed antioxidant activity and increasing EO concentration significantly improved the antioxidant activity. Moreover, nanofibers containing 20, 25, and 30% EO had good antibacterial activity against *E. coli* and *S. aureus*. It can be concluded from these results that the SBS technique can be successfully used for the production of PLA-based nanofiber enriched with EOs, and these nanofibers can be applied not only for drug delivery systems but also for food packaging applications.

Acknowledgements This study was financially supported by the Scientific Research Project Units of Bursa Technical University (200Y007). Part of this study was taken from İklime Özcan's master thesis.

Funding Funding was supported by Bursa Technical University, (Grant No. 200Y007).

References

- Aytac Z, Ipek S, Durgun E, Tekinay T, Uyar T (2017) Antibacterial electrospun zein nanofibrous web encapsulating thymol/cyclodextrin-inclusion complex for food packaging. *Food Chem* 233:117–124. <https://doi.org/10.1016/j.foodchem.2017.04.095>
- Li H, Kochhar JS, Pan J, Chan SY, Kang L (2011) Nano/microscale technologies for drug delivery. *J Mech Med Biol* 11(02):337–367
- Medeiros ES, Glenn GM, Klamczynski AP, Orts WJ, Mattoso LHC (2009) Solution blow spinning: a new method to produce micro- and nanofibers from polymer solutions. *J Appl Polym Sci* 113(4):2322–2330. <https://doi.org/10.1002/app.30275>
- Jiang S, Lv J, Ding M, Li Y, Wang H, Jiang S (2016) Release behavior of tetracycline hydrochloride loaded chitosan/poly(lactic acid) antimicrobial nanofibrous membranes. *Mater Sci Eng, C* 59:86–91. <https://doi.org/10.1016/j.msec.2015.10.005>
- Behrens AM, Casey BJ, Sikorski MJ, Wu KL, Tutak W, Sandler AD, Kofinas P (2014) In situ deposition of PLGA nanofibers via solution blow spinning. *ACS Macro Lett* 3(3):249–254
- Oliveira JE, Moraes EA, Costa RGF, Afonso AS, Mattoso LHC, Orts WJ, Medeiros ES (2011) Nano and submicrometric fibers of poly(D, L-lactide) obtained by solution blow spinning: Process and solution variables. *J Appl Polym Sci* 122(5):3396–3405. <https://doi.org/10.1002/app.34410>
- Oliveira JE, Mattoso LH, Orts WJ, Medeiros ES (2013) Structural and morphological characterization of micro and nanofibers produced by electrospinning and solution blow spinning: a comparative study. *Adv Mater Sci Eng* 2013:1–74
- Oliveira JE, Moraes EA, Marconcini JM, Mattoso LH C, Glenn GM, Medeiros ES (2013) Properties of poly (lactic acid) and poly (ethylene oxide) solvent polymer mixtures and nanofibers made by solution blow spinning. *J Appl Polym Sci* 129(6):3672–3681
- Liu F, Saricaoglu FT, Avena-Bustillos RJ, Bridges DF, Takeoka GR, Wu VCH, Zhong F (2018) Antimicrobial carvacrol in solution blow-spun fish-skin gelatin nanofibers. *J Food Sci* 83(4):984–991. <https://doi.org/10.1111/1750-3841.14076>
- Liu F, Avena-Bustillos RJ, Woods R, Chiou BS, Williams TG, Wood DF, McHugh TH (2016) Preparation of zein fibers using solution blow spinning method. *J Food Sci* 81(12):N3015–N3025
- Pang X, Zhuang X, Tang Z, Chen X (2010) Polylactic acid (PLA): research, development and industrialization. *Biotechnol J* 5(11):1125–1136
- Souza MA, Oliveira JE, Medeiros ES, Glenn GM, Mattoso LH (2015) Controlled release of linalool using nanofibrous membranes of poly (lactic acid) obtained by electrospinning and solution blow spinning: a comparative study. *J Nanosci Nanotechnol* 15(8):5628–5636
- Bonan RF, Bonan PRF, Batista AUD, Sampaio FC, Albuquerque AJR, Moraes MCB, Oliveira JE (2015) In vitro antimicrobial activity of solution blow spun poly(lactic acid)/polyvinylpyrrolidone nanofibers loaded with copaiba (*Copaifera* sp) oil. *Mater Sci Eng* 48:372–377. <https://doi.org/10.1016/j.msec.2014.12.021>
- Nepomuceno NC, Barbosa MA, Bonan RF, Oliveira JE, Sampaio FC, Medeiros ES (2018) Antimicrobial activity of PLA/PEG nanofibers containing terpinen-4-ol against *Aggregatibacter actinomycetemcomitans*. *J Appl Polym Sci* 135(6):45782. <https://doi.org/10.1002/app.45782>
- Yavari Maroufi L, Ghorbani M, Mohammadi M, Pezeshki A (2021) Improvement of the physico-mechanical properties of antibacterial electrospun poly lactic acid nanofibers by incorporation of guar gum and thyme essential oil. *Coll Surfaces A* 622:126659. <https://doi.org/10.1016/j.colsurfa.2021.126659>
- Pelissari FM, Andrade-Mahecha MM, Sobral PJ, d. A., & Menegalli, F. C. (2013) Comparative study on the properties of flour and starch films of plantain bananas (*Musa paradisiaca*). *Food Hydrocoll* 30(2):681–690. <https://doi.org/10.1016/j.foodhyd.2012.08.007>
- ASTM (2001) Standart test method for tensile properties of thin plastic sheeting. American Society for Testing and Materials (ASTM), Philadelphia
- Pirinc FT, Dagdelen AF, Saricaoglu FT (2021) Mechanical, barrier, thermal, and microstructural properties of poly (lactic acid) and gelatin-beeswax emulsion bi-layer films. *J Food Process Preserv* 45(12):e16073. <https://doi.org/10.1111/jfpp.16073>
- McHugh TH, Avena-Bustillos R, Krochta JM (1993) Hydrophilic edible films: modified procedure for water vapor permeability and explanation of thickness effects. *J Food Sci* 58(4):899–903. <https://doi.org/10.1111/j.1365-2621.1993.tb09387.x>
- Lin L, Dai Y, Cui H (2017) Antibacterial poly(ethylene oxide) electrospun nanofibers containing cinnamon essential oil/beta-cyclodextrin proteoliposomes. *Carbohydr Polym* 178:131–140. <https://doi.org/10.1016/j.carbpol.2017.09.043>
- Picciani PHS, Medeiros ES, Pan Z, Wood DF, Orts WJ, Mattoso LHC, Soares BG (2010) structural, electrical, mechanical, and thermal properties of electrospun poly(lactic acid)/polyaniline blend fibers. *Macromol Mater Eng* 295(7):618–627. <https://doi.org/10.1002/mame.201000019>
- Promnil S, Numpaisal P-O, Ruksakulpiwat Y (2021) Effect of molecular weight on mechanical properties of electrospun poly (lactic acid) fibers for meniscus tissue engineering scaffold. *Materials Today: Proceedings* 47:3496–3499. <https://doi.org/10.1016/j.matpr.2021.03.504>
- Karkhanis SS, Stark NM, Sabo RC, Matuana LM (2018) Water vapor and oxygen barrier properties of extrusion-blown poly (lactic acid)/cellulose nanocrystals nanocomposite films. *Compos A Appl Sci Manuf* 114:204–211
- Yang Z, Shen C, Zou Y, Wu D, Zhang H, Chen K (2021) Application of solution blow spinning for rapid fabrication of Gelatin/Nylon 66 nanofibrous film. *Foods* 10(10):2339
- Zhang H, Zhang C, Wang X, Huang Y, Xiao M, Hu Y, Zhang J (2022) Antifungal electrospinning nanofiber film incorporated with *Zanthoxylum bungeanum* essential oil for strawberry and sweet cherry preservation. *LWT* 169:113992. <https://doi.org/10.1016/j.lwt.2022.113992>
- Miranda KWE, Mattoso LHC, Bresolin JD, Hubinger SZ, Medeiros ES, de Oliveira JE (2019) Polystyrene bioactive nanofibers

- using orange oil as an ecofriendly solvent. *J Appl Polym Sci* 136(15):47337. <https://doi.org/10.1002/app.47337>
27. Adeli H, Khorasani MT, Parvazinia M (2019) Wound dressing based on electrospun PVA/chitosan/starch nanofibrous mats: fabrication, antibacterial and cytocompatibility evaluation and in vitro healing assay. *Int J Biol Macromol* 122:238–254. <https://doi.org/10.1016/j.ijbiomac.2018.10.115>
 28. Agrawal P, Pramanik K (2016) Chitosan-poly (vinyl alcohol) nanofibers by free surface electrospinning for tissue engineering applications. *Tissue Eng Regen Med* 13(5):485–497
 29. Alavarse AC, de Oliveira Silva FW, Colque JT, da Silva VM, Prieto T, Venancio EC, Bonvent J-J (2017) Tetracycline hydrochloride-loaded electrospun nanofibers mats based on PVA and chitosan for wound dressing. *Mater Sci Eng, C* 77:271–281
 30. Milleret V, Hefti T, Hall H, Vogel V, Eberli D (2012) Influence of the fiber diameter and surface roughness of electrospun vascular grafts on blood activation. *Acta Biomater* 8(12):4349–4356
 31. Saricaoglu FT, Turhan S (2019) Physical, chemical, thermal and microstructural characterization of edible films from mechanically deboned chicken meat proteins. *J Polym Environ* 27(5):1071–1085. <https://doi.org/10.1007/s10924-019-01410-5>
 32. Zhu P, Zhang X, Wang Y, Li C, Wang X, Tie J, Wang Y (2021) Electrospun polylactic acid nanofiber membranes containing *Caparis spinosa* L. extracts for potential wound dressing applications. *J Appl Polym Sci* 138(32):50800. <https://doi.org/10.1002/app.50800>
 33. Mushtaq M, Wasim M, Naeem MA, Khan MR, Yue S, Saba H, Wei Q (2020) Composite of PLA nanofiber and hexadecyl trimethyl-ammonium chloride-modified montmorillonite clay: fabrication and morphology. *Coatings* 10(5):484
 34. Zhang G, Zhang J, Zhou X, Shen D (2003) Miscibility and phase structure of binary blends of polylactide and poly (vinylpyrrolidone). *J Appl Polym Sci* 88(4):973–979
 35. Deng L, Li Y, Feng F, Wu D, Zhang H (2019) Encapsulation of allopurinol by glucose cross-linked gelatin/zein nanofibers: characterization and release behavior. *Food Hydrocolloids* 94:574–584
 36. Nagy ZK, Balogh A, Vajna B, Farkas A, Patyi G, Kramarics Á, Marosi G (2012) Comparison of electrospun and extruded Soluplus®-based solid dosage forms of improved dissolution. *J Pharm Sci* 101(1):322–332
 37. Wang D, Sun Z, Sun J, Liu F, Du L, Wang D (2021) Preparation and characterization of polylactic acid nanofiber films loading Perilla essential oil for antibacterial packaging of chilled chicken. *Int J Biol Macromol* 192:379–388. <https://doi.org/10.1016/j.ijbiomac.2021.09.190>
 38. Mori CL, dos Passos NA, Oliveira JE, Altoé TF, Mori FA, Mattoso LHC, Tonoli GHD (2015) Nanostructured polylactic acid/candeia essential oil mats obtained by electrospinning. *J Nanomater* 2015:1–9
 39. Ciko L, Andoni A, Ylli F, Plaku E, Taraj K (2016) A study on oil extraction from albanian chamomile and characterization by IR spectroscopy. *J Int Environ Appl Sci* 11(2):154–158
 40. Khosh Manzar M, Mohammadi M, Hamishehkar H, Piruzifard MK (2021) Nanophytosome as a promising carrier for improving cumin essential oil properties. *Food Biosci* 42:101079. <https://doi.org/10.1016/j.fbio.2021.101079>
 41. Arrieta MP, López J, Ferrándiz S, Peltzer MA (2013) Characterization of PLA-limonene blends for food packaging applications. *Polym Testing* 32(4):760–768. <https://doi.org/10.1016/j.polymertesting.2013.03.016>
 42. Trifan A, Zengin G, Brebu M, Skalicka-Woźniak K, Luca SV (2021) Phytochemical characterization and evaluation of the antioxidant and anti-enzymatic activity of five common spices: focus on their essential oils and spent material extractives. *Plants* 10(12):2692
 43. Akhter R, Masoodi FA, Wani TA, Rather SA (2019) Functional characterization of biopolymer based composite film: incorporation of natural essential oils and antimicrobial agents. *Int J Biol Macromol* 137:1245–1255. <https://doi.org/10.1016/j.ijbiomac.2019.06.214>
 44. Saricaoglu FT, Turhan S (2020) Physicochemical, antioxidant and antimicrobial properties of mechanically deboned chicken meat protein films enriched with various essential oils. *Food Packag Shelf Life* 25:100527. <https://doi.org/10.1016/j.fpsl.2020.100527>

Publisher's Note Springer Nature remains neutral with regard to jurisdictional claims in published maps and institutional affiliations.

Springer Nature or its licensor (e.g. a society or other partner) holds exclusive rights to this article under a publishing agreement with the author(s) or other rightsholder(s); author self-archiving of the accepted manuscript version of this article is solely governed by the terms of such publishing agreement and applicable law.